The escalatory Red Queen

Antoine Persoons, Katherine Hayden, Bénédicte Fabre, Pascal Frey, Stéphane de Mita, Aurélien Tellier, Fabien Halkett

▶ **To cite this version:**

Antoine Persoons, Katherine Hayden, Bénédicte Fabre, Pascal Frey, Stéphane de Mita, et al.. The escalatory Red Queen: Population extinction and replacement following arms race dynamics in poplar rust. Molecular Ecology, 2017, 26 (7), pp.1902-1918. 10.1111/mec.13980 . hal-01564550

HAL Id: hal-01564550
https://hal.science/hal-01564550

Submitted on 18 Jul 2017

HAL is a multi-disciplinary open access archive for the deposit and dissemination of scientific research documents, whether they are published or not. The documents may come from teaching and research institutions in France or abroad, or from public or private research centers.

L'archive ouverte pluridisciplinaire **HAL**, est destinée au dépôt et à la diffusion de documents scientifiques de niveau recherche, publiés ou non, émanant des établissements d'enseignement et de recherche français ou étrangers, des laboratoires publics ou privés.

MOLECULAR ECOLOGY

Molecular Ecology (2017) **26**, 1902–1918 doi: 10.1111/mec.13980

MICROBIAL LOCAL ADAPTATION

The escalatory Red Queen: Population extinction and replacement following arms race dynamics in poplar rust

ANTOINE PERSOONS,*[1] KATHERINE J. HAYDEN,*[2] BÉNÉDICTE FABRE,* PASCAL FREY,* STÉPHANE DE MITA,* AURÉLIEN TELLIER† and FABIEN HALKETT*

UMR IAM, INRA, Université de Lorraine, 54000 Nancy, France, †Section of Population Genetics, Center of Life and Food Sciences Weihenstephan, Technische Universität München, 85354 Freising, Germany,

Abstract

Host–parasite systems provide convincing examples of Red Queen co-evolutionary dynamics. Yet, a key process underscored in Van Valen's theory – that arms race dynamics can result in extinction – has never been documented. One reason for this may be that most sampling designs lack the breadth needed to illuminate the rapid pace of adaptation by pathogen populations. In this study, we used a 25-year temporal sampling to decipher the demographic history of a plant pathogen: the poplar rust fungus, *Melampsora larici-populina*. A major adaptive event occurred in 1994 with the breakdown of R7 resistance carried by several poplar cultivars widely planted in Western Europe since 1982. The corresponding virulence rapidly spread in *M. larici-populina* populations and nearly reached fixation in northern France, even on susceptible hosts. Using both temporal records of virulence profiles and temporal population genetic data, our analyses revealed that (i) R7 resistance breakdown resulted in the emergence of a unique and homogeneous genetic group, the so-called cultivated population, which predominated in northern France for about 20 years, (ii) selection for Vir7 individuals brought with it multiple other virulence types via hitchhiking, resulting in an overall increase in the population-wide number of virulence types and (iii) – above all – the emergence of the cultivated population superseded the initial population which predominated at the same place before R7 resistance breakdown. Our temporal analysis illustrates how antagonistic co-evolution can lead to population extinction and replacement, hence providing direct evidence for the escalation process which is at the core of Red Queen dynamics.

Keywords: gene-for-gene interaction, genetic hitchhiking, parasite, Red Queen hypothesis, temporal sampling

Received 29 July 2016; revision accepted 15 December 2016

Introduction

Since the publication of the 'new evolutionary law' by Van Valen more than 40 years ago (Van Valen 1973), the metaphor of the Red Queen has fostered numerous developments in evolutionary biology (Brockhurst *et al.* 2014). Parasites have been credited as primary drivers for the evolution of sexual reproduction (Lively *et al.* 1990; Busch *et al.* 2004; Lively 2010) and have illustrated co-evolutionary cycles expected with the so-called Red Queen dynamics (e.g. Dybdahl & Lively 1998; Thrall *et al.* 2001, 2012; Decaestecker *et al.* 2007; Betts *et al.* 2014). Yet to our knowledge, no study has explicitly tested the core hypothesis of Van Valen (1973): antagonistic co-evolution can lead to extinction (Dawkins & Krebs 1979). In this article, we aim to benefit from a comprehensive and long-lasting survey to document population extinction in a plant pathogen species facing strong selection exerted by host resistance.

Correspondence: Fabien Halkett, Fax: +33 3 83 39 40 69; E-mail: fabien.halkett@inra.fr

[1]Present address: Earlham Institute, Norwich Research Park Innovation Centre, Colney Ln, Norwich NR4 7UH, UK

[2]Present address: Royal Botanic Garden Edinburgh, 20A Inverleith Row, Edinburgh EH3 5LR, UK

© 2016 John Wiley & Sons Ltd

Plant systems lend themselves to studying the occurrence and the mechanisms of extinction events due to host–parasite dynamics, as much is known on the molecular basis of the interactions. In plants, major resistance to fungal pathogens relies on the so-called gene-for-gene interaction (Flor 1971). In the simplest set-up, the outcome of infection is determined by one locus in the plant (the resistance (R) gene) and in the pathogen (the infectivity gene). One allele of the pathogen infectivity gene, which is termed hereafter as the avirulence (*Avr*) allele as in the plant pathology literature, is recognized by plants harbouring a matching resistance allele at the corresponding R-gene. Once the pathogen is recognized, a defence response is triggered (Jones & Dangl 2006). If plants harbour a susceptibility allele – or if the pathogen has the alternative virulence allele – infection occurs. In many cultivated crop species, such major resistance genes have been favoured in selection by plant breeders because they provide complete control of the disease. However, despite the potential for great efficiency, gene-for-gene resistance may be quickly broken down, as a single mutation in the pathogen *Avr* allele can be sufficient to break or change its functionality and impair recognition of the plant R-gene, thereby restoring virulence (Schulze-Lefert *et al*. 1997). In this case, the so-called resistance breakdown is accompanied by the possible fixation of the virulence allele in the parasite population. Infectivity loci code for pathogenicity factors, also known as effectors, which accordingly contribute to the success of pathogen infection. Virulent individuals are often shown to exhibit a fitness penalty (the so-called virulence cost) when compared to individuals harbouring the *Avr* allele on susceptible plants (Huang *et al*. 2006; Bahri *et al*. 2009a; Montarry *et al*. 2010).

Over time, a wide range of dynamics in changes in allele frequencies in plant and pathogen populations can be observed. At one end of the spectrum, we find trench-warfare dynamics, in which polymorphism is maintained in the plant and pathogen populations, as has been shown in several wild species (Thrall *et al*. 2001, 2012). At the other end, arms races can occur with recurrent fixation of new resistance and virulence alleles in plant and pathogen populations. The ecological conditions and life history traits, such as host perenniality, generating these dynamics have been shown theoretically (Tellier & Brown 2007, 2009; Brown & Tellier 2011). In agriculture, arms races are expected to occur because of the synchronization between plant and pathogen life cycles (Brown & Tellier 2011). The temporal dynamics of these selective sweep events are driven in large part by the mutation rate in the pathogen population (Tellier *et al*. 2014), and pathogens should show clearer signatures of selection at co-evolving genes than the hosts (Tellier *et al*. 2014). Recent findings support the theory with effector genes showing elevated levels of nonsynonymous polymorphisms (Poppe *et al*. 2015). Theory also predicts that extinction of host and/or parasite populations following co-evolution should occur under arms races rather than under trench warfare scenarios (Dawkins & Krebs 1979; Brockhurst *et al*. 2014). Therefore, understanding the mechanisms linking allele fixation in host and pathogen populations and the extinction of a host or parasite species (or population at the intraspecific level) is of fundamental importance for testing the Red Queen predictions.

In this study, we investigate the temporal changes in population structure in the poplar rust pathogen, *Melampsora larici-populina*, which underwent a severe selection event in poplar-cultivating areas (Xhaard *et al*. 2011). Worldwide, *Melampsora* spp. (Basidiomycota, Pucciniales) are the most damaging pathogens of poplars (Vialle *et al*. 2011), and *M. larici-populina* is the largest problem in European poplar plantations (Frey *et al*. 2005). Poplars are particularly susceptible to *M. larici-populina* because of their intensive monoclonal cultivation spanning several decades and the probable counterselection of nonspecific resistance traits during breeding (Gérard *et al*. 2006). Eight resistances (R1 to R8) have been described in poplar so far (Pinon & Frey 2005). Most of them have been deployed in European plantations, and all have been overcome by *M. larici-populina* (Pinon & Frey 2005). The most economically damaging resistance breakdown occurred when the widely planted R7 resistance was overcome and led to the invasion of France by Vir7 *M. larici-populina* individuals (Fig. 1). Several poplar cultivars bear the R7 resistance, among which *Populus* × *interamericana* 'Beaupré' was the most popular, accounting for 57% of the stems planted in France in 1996, and as much as 80% in northern France (Pinon & Frey 2005). Conversely, other resistance types (including R1 to R5) have been planted at a low and constant frequency since the 1950s (Pinon & Frey 2005). The first report of R7 resistance breakdown occurred in 1994 in Belgium and northern France (Pinon & Frey 2005). In fewer than 5 years, Vir7 individuals spread all over Western Europe and went on to cause very destructive epidemics on all cultivated poplar stands, whether or not they carried R7 resistance. It is noteworthy that unlike annual crops, poplar cultivation has a rotation time of 15–25 years. Even while planting of 'Beaupré' rapidly collapsed after R7 resistance breakdown and the resulting massive epidemics, this cultivar still predominated poplar plantations of northern France for about 20 years, thus exerting a sustained and strong selection pressure on *M. larici-populina* populations.

A previous population genetic study demonstrated that poplar rust populations have been greatly impacted

© 2016 John Wiley & Sons Ltd

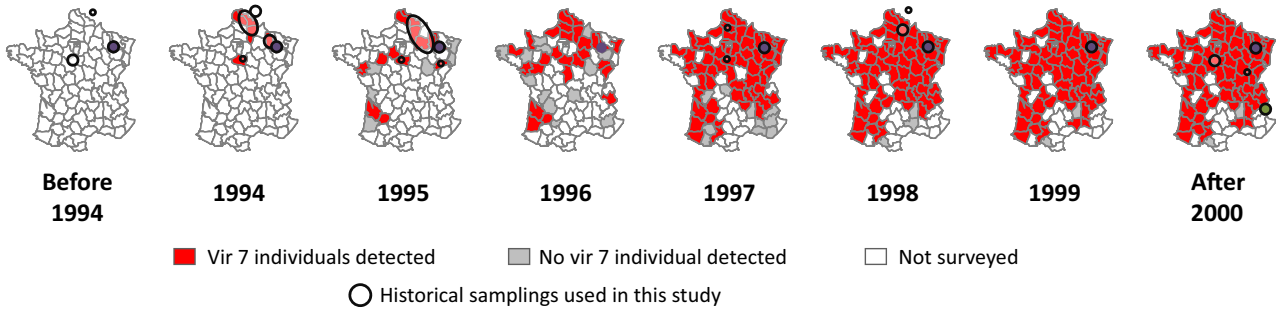

Fig. 1 Illustration of the spread of Vir7 individuals in France (after Pinon *et al.* 1998) and associated sampling design. Large circles indicate population sampling, small circles indicate individual sampling, and ellipses indicate multiple sampling sites. Filled circles indicate when the sample has been phenotyped (in Nancy and Prelles). In 1996, individuals have only been phenotyped. The survey of the spread of Vir7 individual stopped in 1999. [Colour figure can be viewed at wileyonlinelibrary.com]

by this long-lasting selection pressure (Xhaard *et al.* 2011). The present population structure of *M. larici-populina* in France is best explained by only two major genetic groups (hereafter called populations). The most abundant type includes nearly all Vir7 individuals and displays the hallmarks of a history of strong selection. It was thus named the cultivated population. This population predominates in northern France even on hosts not carrying R7 resistance. The second population is closer to genetic equilibrium and predominates in southern France, especially in some refuges, like the upper Durance River valley in the Alps (Xhaard *et al.* 2012). While the Xhaard *et al.* (2011) study provides strong evidence that the R7 resistance breakdown was at the origin of the cultivated population, it was not possible to date the foundation of this population as this study was based on a single time point collection, in 2009.

In the study presented here, we demonstrate, using a retrospective analysis, a genetically variable pathogen population being driven to extinction and replaced, consistent with arms race dynamics. We assembled a comprehensive genetic and phenotypic database from a historical collection of *M. larici-populina* sampled in France and Belgium. Phenotype data consisted of nearly 7000 individuals typed for their virulence profile between 1992 and 2012. A selection of nearly 600 isolates representative of a broader collection built between 1982 and 2011 was genotyped using 25 microsatellite markers. The combined analysis of genetic data and virulence profiles has been proven useful to unravel the temporal evolution following major resistance breakdown events (Hovmøller *et al.* 2016). Here, phenotypic and genotypic data sets were analysed using similar methodologies (clustering followed by temporal characteristics analyses); so that the results complement each other. Our objectives were the following: (i) to trace back the origin of the cultivated rust population, suspected to have been founded by the major R7 resistance breakdown event, (ii) to examine the temporal evolution of its genetic and phenotypic characteristics since its foundation and check for genetic consistency across years and (iii) to search for the pre-existing population and quantify the magnitude of the shift in population structure caused by such a major selection event.

Materials and methods

Melampsora larici-populina life cycle and sampling strategy

Melampsora larici-populina exhibits a host-alternating life cycle; that is, it requires two hosts each year to be completed. Briefly, this fungal species reproduces asexually on poplar leaves during summer and autumn – where it causes epidemics – and then switches to a sexual phase, which takes place on larch (Xhaard *et al.* 2011). As a result of this obligate annual sexual reproduction, high levels of genotypic diversity are observed in all locations, even when individuals are collected at the end of the asexual phase (Gérard *et al.* 2006; Barrès *et al.* 2008), as expected for cyclical parthenogenetic organisms (Halkett *et al.* 2005; Rouger *et al.* 2016). In addition, during sexual reproduction, the gametes produced in spring on poplar leaf litter are wind-dispersed to infect larch needles (where the sexual reproduction is completed by the production of sexual organs and subsequent plasmogamy). This part of the life cycle ensures large genetic reshuffling among individuals each year. Such a life cycle thus fosters gene flow and prevents local/host adaptation at small spatial scales (Barrès *et al.* 2008; Gilabert *et al.* 2009). In accordance, previous population genetic studies on *M. larici-populina* revealed a very low level of genetic differentiation between host plants or locations in populations where sexual

© 2016 John Wiley & Sons Ltd

reproduction takes place (Gérard *et al.* 2006; Barrès *et al.* 2008).

Beyond this predominantly sexual life cycle, some individuals can reproduce asexually from year to year, as evidenced from their peculiar genetic profiles (Xhaard *et al.* 2011). Little is known about the evolutionary history of these asexual lineages, but these individuals do not carry Vir 7, indicating their emergence is not linked to the breakdown of R7 resistance. Those individuals were not considered in this study.

The sampling design used in this study relied on the historical monitoring of poplar rust in France (Fig. 1, Table 1) and was based on the previously observed contemporary population structure (predominance of the cultivated population in northern France and persistence of the wild population in some refuges in the south of France). The reference site of Prelles, a wild poplar stand located in the French Alps (Xhaard *et al.* 2012), was thus used as an outgroup to contrast the temporal evolution of *M. larici-populina* populations that occurred in northern France (Fig. 1).

Table 1 Summary of *M. larici-populina* collection sampling. The numbers in brackets indicate the few individuals collected on cultivated poplars bearing the Resistance 7; otherwise, all were collected on fully susceptible hosts (either larch or poplar)

	Cultivated poplar areas		Wild stand	
Year	Nancy	Others[†]	Prelles	Total
1982	–	1	–	1
1985	1	–	–	1
1988	4	3	–	7
1992	22[‡]	5	–	27
1993	30[‡]	–	–	30
1994	14	30 (27)	–	44
1995	11[‡] (1)	18 (18)	–	29
1996	3[‡]	–	–	3
1997	14[‡]	2	–	16
1998	15 (2)	18 (17)	–	33
1999	11[‡]	–	–	11
2000	1	–	–	1
2001	14[‡]	1	–	15
2002	7[‡]	1	–	8
2003	8[‡]	–	–	8
2004	6[‡]	–	–	6
2005	–	3[§]	–	3
2006	7		–	7
2007	15[§]	–	–	15
2008	29[§]	–	76	105
2009	28[§]	24	63	115
2011	31	28	50[‡]	109
Total	271	134	189	594

[†]Collection events gathering individuals from different sampling locations in northeastern France (excluding Nancy) and Belgium.
[‡]Mixture of larch and poplar samplings.
[§]Sampling on larch only.

Virulence analysis

Sampling and virulence profile assessment. Virulence analysis relied on a comprehensive and long-term phenotypic survey of poplar rust at INRA Nancy. First, rust isolates were sampled each year in an experimental poplar nursery at the INRA campus from 1992 to 2012 (mean sample size of 150 isolates). This experimental site is designed to reflect the overall composition of *M. larici-populina* populations present in poplar cultivation areas. Second, for the sake of comparison, we included virulence data from isolates collected in the reference site of Prelles (poplar-larch native sympatry area, Xhaard *et al.* 2011, 2012). Isolates from Prelles were collected from 2004 to 2012 (mean sample size of 130 isolates).

Melampsora larici-populina isolates were collected from symptomatic leaves of either the universally susceptible poplar cultivar *Populus* × *euramericana* 'Robusta' (summer and autumn collections at INRA nursery), the universally susceptible *Populus nigra* (summer and autumn collections at Prelles), or European larch (*Larix decidua*), the alternate host (spring collections at INRA nursery and at Prelles). A single sporulating lesion was isolated from each poplar leaf or larch needle and grown on fresh leaf discs of 'Robusta' in controlled conditions as described by Gérard *et al.* (2006). This procedure ensures that a single genotype is isolated (Xhaard *et al.* 2011). Sampling from different leaves also minimizes the risk that clone mates are resampled (Barrès *et al.* 2012).

After collection, isolates were inoculated on a differential set of eight poplar cultivars, each bearing a single qualitative resistance, to determine which virulence type(s) they possessed, as described in Barrès *et al.* (2008). In total, nearly 7000 individuals from 44 samples (combinations of sampling year and site) were analysed.

Virulence types and virulence profile analysis. Information on all virulence types was combined to determine the virulence profile of each individual (i.e. combination of virulence types, also called pathotype in the phytopathology literature). This profile is analogous to the multilocus genetic profile that results from microsatellite analysis.

From virulence profile frequencies in each sample, we calculated both an evenness index (E) and a richness index (Shannon relative index, H_{SR}) to illustrate the relative abundance of profiles and mean profile diversity,

© 2016 John Wiley & Sons Ltd

respectively (Barrès *et al.* 2008). The evenness index (E) is derived from the Simpson's index corrected for sample size after Fager (1972). We first calculated the complement of Simpson's index (D) for each sample as $D = 1 - \sum_i k_i(k_i - 1)/N_p(N_p - 1)$, where k_i is the number of isolates of profile i and N_p is the number of isolates analysed for virulence in the sample. Then, we calculated E, which is not influenced by sample size, as $E = (D - D_{\min})/(D_{\max} - D_{\min})$ where $D_{\min} = [(n_p - 1)(2N_p - n_p)]/[N_p(N_p - 1)]$ and $D_{\max} = [(n_p - 1)N_p]/[n_p(N_p - 1)]$, where n_p is the number of profiles found in the sample. The richness index H_{SR} is derived from the Shannon's index corrected for sample size and calculated as follows: $H_{SR} = -\sum_i (k_i/N_p)\ln(k_i/N_p)/\ln(N_p)$. We also computed an index of virulence profile complexity (P_C) defined as the mean number of virulence types carried by a single isolate (Andrivon & De Vallavieille-Pope 1995). All analyses were performed using R (R Core Team 2014).

Individual clustering was first assessed via discriminant analysis of principal components using the R package ADEGENET (Jombart *et al.* 2010), with virulence types coded as haploid, presence–absence characters. Second, population samples and virulence profiles were grouped according to a hierarchical clustering procedure and visualized using the heatmap function in base R (R Core Team 2014) without clone correction or stratification of sampling sites and dates.

Population genetic analyses

Sampling strategy. Sampling relied on a large collection of *M. larici-populina* isolates sampled from 1982 to 2012. This collection was initially built with the aim of representing the diversity of rust isolates, hence maximizing sampling locations and poplar cultivars of origin with the cost of reduced sample sizes. It was nonetheless possible to define, based on this collection, a coherent sampling scheme focusing on some locations regularly sampled through time, in particular in the experimental poplar nursery at INRA Nancy (Table 1). We enriched this sampling scheme with other sampling sites and years of collection, to provide a broad picture of the temporal evolution in rust population genetic structure before and after the R7 resistance breakdown event. To reflect the composition of the population without a selective filter at a given site and year, this sampling was primarily performed on susceptible poplar cultivars as in Xhaard *et al.* (2011). Some individuals collected on R7 poplar cultivars just after the discovery of the resistance breakdown were included to further examine the genotypes of the very first Vir7 individuals (Table 1, in brackets). To compare the dynamics in these samples to a largely non-Vir7 outgroup, we analysed the genotypes of 189 individuals collected in 2008, 2009 and 2011 from Prelles, the reference site for the wild population (Xhaard *et al.* 2011). The 2009 sampling of 115 isolates in all three locations was previously reported in Xhaard *et al.* (2011). In total, we analysed the genotype of 594 individuals, half of them being sampled at Nancy.

Individual isolation. Individuals were isolated from rust-infected poplar leaves collected in the field (Table 1), according to the protocol detailed above. For samplings collected earlier than 2004, a mono-uredinial protocol (ensuring that a single genotype per sampled leaf is isolated and multiplied) was not strictly observed. As isolates were kept alive in liquid nitrogen from the time they were collected, those older isolates were multiplied again on fresh leaf discs of 'Robusta' and a first batch of microsatellite genotyping was performed to check genotype purity. In the case of ambiguous genotypic profile, isolates were purified by picking a single spore from a sporulating lesion to start a new multiplication cycle on 'Robusta'. After multiplication, leaf discs of 'Robusta' were frozen and stored at −20 °C until DNA extraction.

Microsatellite genotyping. DNA was extracted using the BioSprint 96 DNA plant kit used in combination with the BioSprint 96 automated workstation (Qiagen®) following the BS96-DNA-plant protocol. Individuals were genotyped with a set of 25 microsatellite markers: MLP12 (Barrès *et al.* 2008), MLP49, MLP50, MLP54, MLP55, MLP56, MLP57, MLP58, MLP59, MLP66, MLP68, MLP71, MLP73, MLP77, MLP82, MLP83, MLP87, MLP91, MLP92, MLP93, MLP94, MLP95, MLP96, MLP97, MLP100 (Xhaard *et al.* 2009, 2011). Microsatellite markers were amplified by multiplex PCR, using the Multiplex PCR Kit (Qiagen®) as detailed in Xhaard *et al.* (2011). Three multiplex PCRs were run, comprising eight, seven and nine loci, respectively (Xhaard *et al.* 2011). PCR products from the three multiplex reactions (3 μL PCR1, 4 μL PCR2 and 5 μL PCR3) were pooled and loaded on an ABI 3730 Genetic Analyzer (Applied Biosystems). Fragment analysis was performed by the Genoscreen Company. Fragments were sized with a LIZ-1200 size standard, and alleles were scored using GENEMAPPER 4.0 (Applied Biosystems). Individuals for which more than six loci failed to amplify were removed for further analyses.

Population structure. We first investigated the population genetic structure of the temporal samples of *M. larici-populina* using the Bayesian clustering method implemented in TESS (Chen *et al.* 2007; Durand *et al.*

© 2016 John Wiley & Sons Ltd

2009). We used the model with admixture, which estimates putative multiple ancestry of individuals. The membership coefficient q to a given cluster is defined as the fraction of the genome that originates from this ancestral population. We used the conditional autoregressive (CAR) Gaussian model of admixture with 100 000 MCMC iterations after the burn-in of 20 000 iterations. We performed ten independent runs for each value of the maximal number of ancestral populations (K_{max}) ranging from 2 to 10. To choose the value of K_{max} that best suits the genetic data, TESS computes the deviance information criterion (DIC) for each run (a procedure similar to the ΔK criterion traditionally used for STRUCTURE (Evanno *et al.* 2005)). The DIC is an index of the model deviance penalized by its complexity (Spiegelhalter *et al.* 2002). The lower the DIC value, the higher the confidence in the model. Moreover, the strength of the TESS method is that the number of clusters (K_{max}) assumed in a simulation run is the upper (not mandatory) number of ancestral populations. The hierarchical mixture algorithm implemented in TESS does not force individuals' genomes to be split in K_{max} populations, so that empty clusters can appear if the population structure is already well explained by fewer clusters. In addition to the analysis of the decrease of DIC values, we also examined how the partition of individuals' genomes evolves when letting the number of clusters vary to select the most likely number of ancestral populations. Then, we fixed a threshold at $q > 0.75$ to assign individuals to a given ancestral population.

We also analysed population structure using Discriminant Analysis of Principal Components (DAPC) implemented in ADEGENET package in R (Jombart *et al.* 2010). This nonparametric approach is complementary to Bayesian clustering analysis as it does not rely on a particular genetic model. DAPC analyses were conducted following the procedure detailed in the ADEGENET tutorial for DAPC (Jombart & Collins 2015).

Population genetic analyses. We computed summary statistics of genetic variability within populations identified using Bayesian clustering methods. Our analysis is based on 24 population samples, with at least six individuals sampled per location and/or year (mean sample size of 14 individuals). Expected (H_E) and observed (H_O) heterozygosities were calculated with GENETIX (4.05) (Belkhir *et al.* 1996-2004). We reported the unbiased estimate of H_E calculated following Nei (1978). We calculated allelic richness (A_r) using FSTAT version 2.9.3 (Goudet 1995) that implements a rarefaction procedure to account for differences in sample size. We reported these two estimates of gene diversity as they can vary differently depending on the demographic regime (Cornuet & Luikart 1996). The partitions of genetic variability at the individual (F_{IS}) and population sample (F_{ST}) levels were estimated according to Weir and Cockerham (Weir & Cockerham 1984) using FSTAT. Given the overall small sample size, F_{IS} values have to be interpreted with caution. Deviation from HW equilibrium expectations (heterozygote excess and deficit) was thus not based on F_{IS} distributions but on the genotypic counts. We used the Markov chain algorithm of GENEPOP (Rousset 2008) to estimate the P-values for the Fisher's exact test (MC parameters: dememorization, 2000; number of batches, 250; iterations per batch, 2000). Linkage disequilibrium was estimated through the multilocus index of association corrected for the number of loci (rbarD) calculated using MULTILOCUS (Agapow & Burt 2001). Significance of the departure from random association of alleles across loci was assessed by bootstrapping alleles among individuals 10 000 times.

Tests for demographic equilibrium. Within-sample tests for mutation–drift equilibrium were performed with BOTTLENECK (Piry *et al.* 1999). This method relies on the fact that populations that have recently experienced a reduction in population size should exhibit larger values of gene diversity (i.e. heterozygosity level) than expected from the number of alleles at mutation–drift equilibrium (Cornuet & Luikart 1996). Tests were performed assuming the two-phase mutational model (TPM) that better suits microsatellite markers. We allowed for 30% multistep changes in the TPM (default proportion). Analyses were performed with 10 000 iterations of the coalescent process. Bottleneck probability was assessed using one-tailed Wilcoxon signed rank tests for heterozygosity excess (the most powerful test considering our limited number of markers (Luikart & Cornuet 1998)).

Analysis of isolation by time. To test the temporal evolution of allelic frequencies, we used an analog of isolation-by-distance analysis, here applied to time-restricted gene flow: the so-called isolation by time (IBT, Hendry & Day 2005). This amounts to performing Mantel tests between matrices of pairwise genetic distances between population samples and temporal distance, calculated as the number of years that separate the samples. We used the 'isolde' algorithm implemented in GENEPOP (Rousset 2008), with $F_{ST}/(1-F_{ST})$ as estimate of genetic distances (as is done for IBD analysis (Rousset 1997)). Significance of regression slope was evaluated through 10 000 permutations.

P-value adjustment for multiple testing. To adjust the P-value for multiple tests, we used the false discovery rate (FDR) procedure (Benjamini & Yekutieli 2001), which controls the proportion of significant results ('false discovery rate') instead of controlling the chance

© 2016 John Wiley & Sons Ltd

of making even a single error. The resulting adjusted *P*-values are called *Q*-values. This procedure was implemented in the R package QVALUE (Storey & Tibshirani 2003).

Results

Virulence profile analyses

Variability of virulence profiles. Considering all virulence types (1–8) and all individuals (6494), we identified 120 virulence profiles (of 256 possible combinations). However, due to missing data on Vir6 and Vir8, which were not routinely assayed before 2000, a full virulence profile could only be confidently assigned for individuals sampled later than 2000. To keep the temporal dimension of this analysis, we decided to omit these two virulence types. Focusing on virulence types 1–5 plus 7, we identified 61 virulence profiles, which is nearly the maximum number of possible combinations (64). Considering only the first five virulence types, all 32 possible combinations were sampled. In all cases, virulence combinations were unevenly distributed among individuals, resulting in a typical L-shaped abundance graph (Fig. S1, Supporting information). For example, considering again virulence types 1–5, only eight virulence combinations accounted for nearly 90% of sampled individuals.

Virulence types 1–5 were detected regularly in Nancy from the first sampling date in 1992. In contrast, Vir7 (which was first observed in France in 1994) was absent from earlier samples, and only first observed at very low frequency (0.2% of isolates) in 1996. The frequency began to increase in 1998, rising to 99% in 2005, and dropped slightly afterwards (Fig. 3a). Because this recent and strong pattern would likely dominate analyses of population structure, the following analyses were performed on the basis of virulence types 1–5 only unless otherwise specified.

Virulence profile clustering. The *K*-means procedure implemented in ADEGENET for clustering individuals according to their virulence profile failed to converge. This is not surprising given the large number of individuals under scrutiny and relatively little information provided by the only five first virulence types. Thus, the dimensionality of the vector space (number of centroids) was too high compared with the residual sum of squares.

We thus decided to work directly on the frequencies of virulence profiles within samples. A hierarchical clustering analysis clearly sorted out Prelles and Nancy samplings (Fig. S2, Supporting information). Prelles samples were very similar to each other. Conversely, Nancy samples were much more variable and sorted according to the sampling date. There was no sharp change in virulence profiles but rather a temporal gradient of changes.

Temporal evolution of virulence profiles in Nancy. This temporal change is obvious when focusing on the most abundant virulence profiles (Fig. 2). In Nancy, we observed a large increase in frequency of virulence profile 1-3-4-5 starting from September 1998, the time when Vir7 was increasing in frequency. As illustrated in Fig. 2, this combination of virulence types has hitchhiked on Vir7. In the meantime, virulence profile 2–4 collapsed. Through annual recombination events, Vir2 introgressed into the emerging virulence profile to form the multivirulence 1-2-3-4-5-7 profile. As a consequence

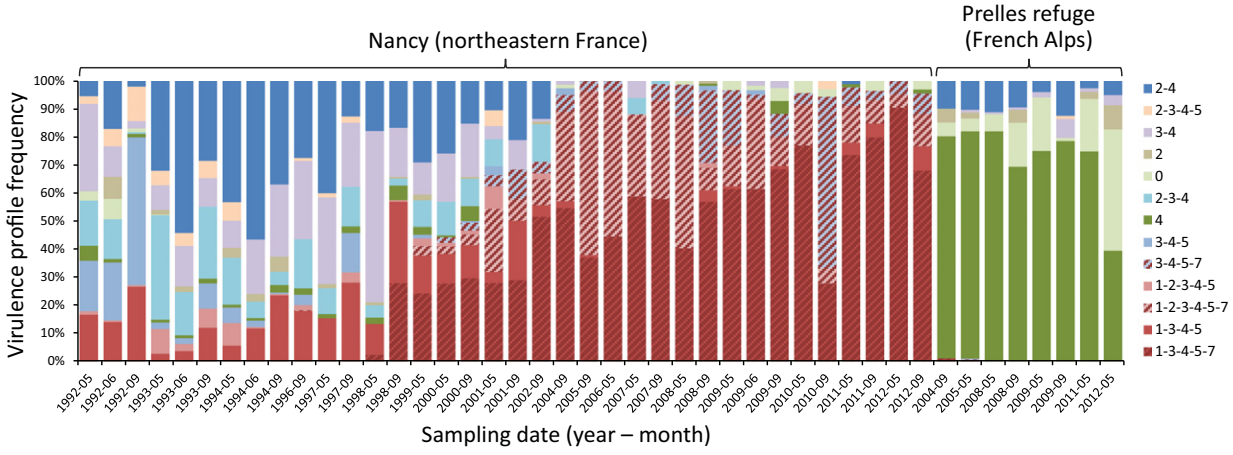

Fig. 2 Barplots of cumulative frequencies of the 13 most represented virulence profiles (nearly 90% of sampled individuals) for all sampling dates and both locations. Colour legend for virulence profiles is listed on the right. Virulence profiles including Vir7 are represented by dashed bars, with the background colour of the Avr7 profile. [Colour figure can be viewed at wileyonlinelibrary.com]

© 2016 John Wiley & Sons Ltd

of virulence types 1, 3, 4, 5 hitchhiking during the emergence of Vir7, virulence profile complexity (the mean number of virulence types carried by an individual) increased from 1998 to 2005 in Nancy (Fig. 3b). During this time, we observed a dominance of virulence profiles 1-3-4-5, then 1-2-3-4-5 (still omitting Vir7), which result in a drop in evenness (Fig. 3c). Interestingly, in recent years, virulence profile complexity decreased (Fig. 3b), although there was a sustained virulence profile richness (Fig. 3d) generated by sexual reproduction.

In contrast to Nancy samples, the Prelles samples showed a near absence of Vir7 individuals, even in the most recent samples. This site exhibited a much reduced virulence profile complexity (0.99 compared with 3.25 on average for Nancy samples), as most individuals were nearly avirulent or bore Vir4 only. Virulence profiles at Prelles were thus less diverse and less evenly distributed (mean richness H_{SR} = 0.18 vs. 0.33; mean evenness E = 0.47 vs. 0.72; see Table S1 (Supporting information) for more information).

Microsatellite profile analyses

Summary of genetic and genotypic diversity. A total of 594 isolates were genotyped with 25 microsatellite loci. Markers amplified correctly (465 individuals without missing data, 1.07% missing data on average, no more than three loci that failed to amplify per individual). Of the 25 markers, three (MLP59, MLP92 and MLP100) displayed drastic deviation from Hardy–Weinberg equilibrium and were removed from the analysis (data not shown). All remaining 22 microsatellite markers were polymorphic, with a number of alleles ranging from 5 to 25 (mean allele number across loci of 10.2). Gene diversity (i.e. expected heterozygosity, H_E) was 0.54 when considering all samples.

Of the 594 individuals analysed, 550 multilocus genotypes (MLGs) were found. Only 30 MLGs were found more than once (mean of 2.5 clonal copies). All clone mates were found on the same site at the same date. One MLG (two copies in Orléans 2011) corresponded to a genotype already described by Xhaard *et al.* (2011) and assigned to the asexual group. These two individuals were removed from this analysis.

Genetic structure. Clustering analysis of the historical collection of *M. larici-populina* samples indicated that the most relevant partition of our genetic data was obtained assuming three populations (Fig. 4 and detailed analysis provided in Annex S1, Supporting information). This partition is biologically realistic and consistent with previous findings: First, individuals sampled in southern France at Prelles formed an initial cluster, which corresponded to the 'wild' population in Xhaard *et al.* (2011). Second, individuals sampled on R7 cultivars from 1994 to 1998 grouped with individuals sampled since 1998 in northeastern France. This cluster corresponded to the 'cultivated' population described in Xhaard *et al.* (2011) and mostly consisted of Vir7 individuals (82% of the tested individuals bear the virulence 7, data not shown). Third, the very first samples of the historical collection (collected from 1992 to 1997 in northern and eastern France before the invasion of Vir7 individuals) formed a third population, which was not sampled, hence not studied, in Xhaard *et al.* (2011). No individual assigned to this population bore the virulence 7 (data not shown). As we found no individuals assigned to this population after 1999, this genetic cluster was named the 'fossil' population.

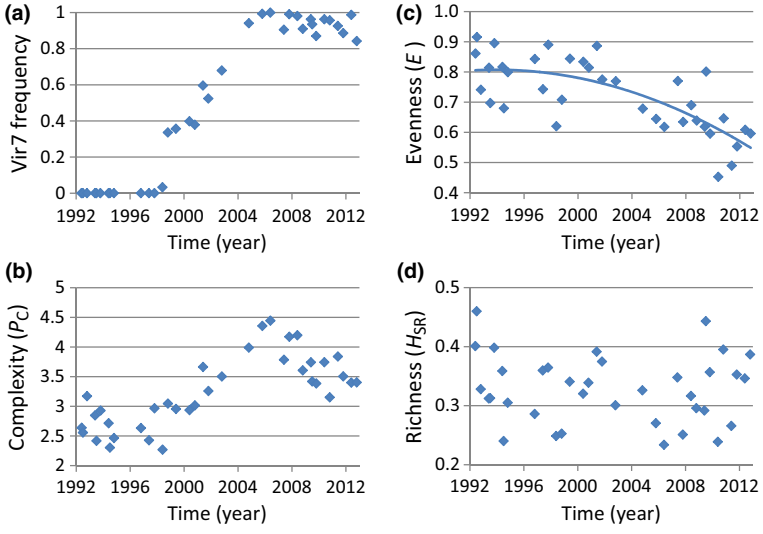

Fig. 3 Temporal evolution of virulence profiles in Nancy: (a) frequency of Vir7 individuals; (b) mean number of virulence types borne by an individual (also called pathotype complexity); (c) evenness of virulence profiles; (d) virulence profile diversity. [Colour figure can be viewed at wileyonlinelibrary.com]

© 2016 John Wiley & Sons Ltd

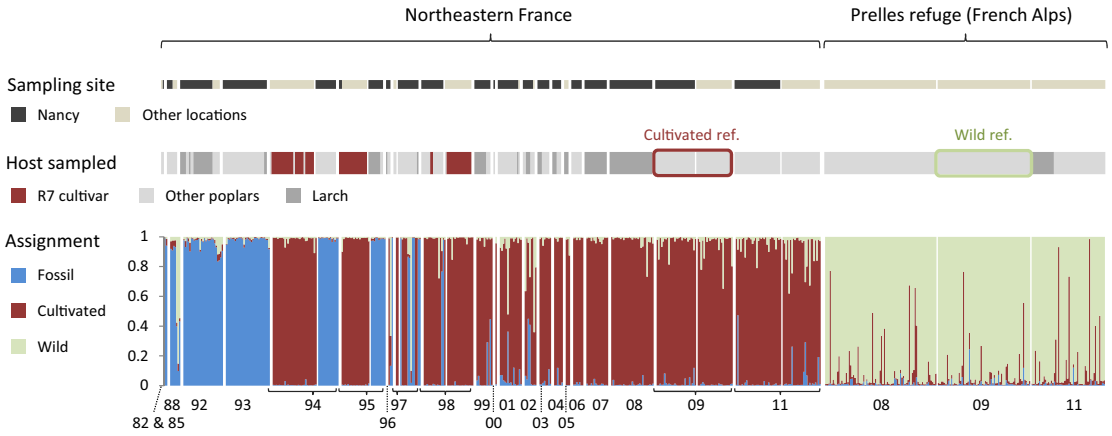

Fig. 4 Barplots of membership probabilities for individual samples of the historical collection (best partition at $K_{max} = 3$). Each vertical bar represents an individual whose genome is partitioned into up to three coloured segments. Segment length is proportional to membership probability to each ancestral population. The type of host sampled and the region of origin are reported above the assignment barplots. Year of sampling (the last two digits) is indicated underneath. Reference individuals from Xhaard *et al.* (2011) are highlighted by two boxes. [Colour figure can be viewed at wileyonlinelibrary.com]

Focusing on the site of Nancy, we clearly observed a replacement of populations between 1997 and 1998, where individuals assigned to the fossil population disappeared as the site became invaded by cultivated individuals. We observed asymmetric gene flow between populations. Few individuals displayed a mixed ancestry with both fossil and cultivated genetic backgrounds (Fig. 4). We found more evidence for gene flow between wild and cultivated populations with individuals sampled in Northern France after 1998 that had high membership probability to the wild population and some individuals sampled in Prelles with mixed ancestry. Note, however, that this result must be interpreted with caution and can simply result from erroneous assignments.

Applying a threshold of $q > 0.75$ on membership coefficients to assign individuals to the three populations led to the exclusion of only 42 individuals. Nearly 92% of the individuals were thus confidently assigned to a genetic population. The level of genetic differentiation among populations was moderate, albeit significant (global $F_{ST} = 0.062$, $P < 0.001$). The fossil population displayed the highest differentiation ($F_{ST} = 0.094$ and 0.072 with cultivated and wild populations, respectively), whereas wild and cultivated populations were more closely related ($F_{ST} = 0.043$).

In the following sections, we focus on the individuals assigned to the three populations only. Those individuals were grouped by site and/or year (within each population). We retained only the collection events with more than six individuals and treated them as samples of the three populations (Table 2).

Genetic characteristics of the three populations. The wild samples displayed the highest genetic diversity. Both allelic richness and heterozygosity levels were significantly higher than those of the cultivated samples (permutation test, $P < 0.001$). No wild sample did significantly depart from genetic equilibrium (no deviation from Hardy–Weinberg proportions nor mutation–drift equilibrium and lack of linkage disequilibrium; Table 2). There was no genetic differentiation among temporal samples (global $F_{ST} = 0.001$).

The fossil population showed the more pronounced deviations from genetic equilibrium (Table 2). Two of five samples displayed significant linkage disequilibrium. This departure from linkage equilibrium was even more pronounced the last time it was sampled, in 1997. The fossil samples also displayed the smallest values of genetic diversity (both allelic richness, *Ar*, and gene diversity, H_E, values).

Most cultivated samples did not significantly depart from genetic equilibrium. The notable exception was the very first sampling of this population in 1994. This sample exhibited the highest value of rbarD and strong departure from HW equilibrium (high F_{IS} value). This sample was also the only one to display a significant *Q*-value for the bottleneck test (Table 2).

Temporal evolution of the cultivated population. The cultivated population presented the highest F_{ST} value among samples (0.022) and the largest heterogeneity in various population genetic indices. We therefore tested for temporal evolution of the genetic characteristics of this population and found a significant isolation by time

© 2016 John Wiley & Sons Ltd

Table 2 Genetic characteristics of the 24 samples defined within the three populations: *Ng*, number of genotyped individuals; MLG, number of distinct multilocus genotypes; *G*/*Ng*, genotypic richness; A_R, allelic richness; H_E, unbiaised estimate of gene diversity; H_O, observed heterozygosity; F_{IS}, within- and among-individual apportionment of gene diversity; HW, deviation from Hardy–Weinberg equilibrium (combined probabilities of the exact HW test using Fisher's method); LD, linkage disequilibrium ($\bar{r}_D$ index value); Bottleneck, probability of the one-tailed Wilcoxon tests for heterozygosity excess under the TPM model

			Genetic diversity									Equilibrium testing		
Year	*Ng*	MLG	*G*/*Ng*	A_R	(se)	H_E	(se)	H_O	(se)	F_{IS}	(se)	HW	LD	Bottleneck
Fossil samples														
1992	22	22	1.000	2.942	(0.875)	0.513	(0.176)	0.465	(0.188)	0.094	(0.209)	0.053	0.017	0.105
1993	30	25	0.828	2.788	(0.833)	0.487	(0.197)	0.442	(0.217)	0.095	(0.195)	0.009	0.028*	0.083
1994	14	11	0.769	2.960	(1.043)	0.486	(0.23)	0.467	(0.265)	0.040	(0.199)	0.723	0.045	0.832
1995	10	10	1.000	2.744	(0.683)	0.498	(0.186)	0.415	(0.216)	0.174	(0.278)	0.180	0.002	0.124
1997	7	7	1.000	2.892	(1.124)	0.490	(0.224)	0.469	(0.268)	0.049	(0.322)	0.919	0.108**	0.380
Overall	83	75	0.902	2.887	(0.849)	0.500	(0.183)	0.452	(0.193)	0.096	(0.160)	0.065	0.013*	0.029
Cultivated samples														
1994†	30	21	0.690	2.738	(0.875)	0.504	(0.199)	0.448	(0.198)	0.114	(0.219)	<0.0001**	0.087***	0.005*
1995†	19	15	0.778	2.903	(1.039)	0.514	(0.235)	0.447	(0.224)	0.133	(0.165)	0.265	0.032*	0.032
1997†	8	8	1.000	2.832	(1.048)	0.485	(0.232)	0.459	(0.258)	0.058	(0.268)	0.647	−0.010	0.684
1998*a*	13	13	1.000	2.984	(1.093)	0.533	(0.231)	0.510	(0.244)	0.045	(0.185)	0.033	0.011	0.056
1998*b*	17	17	1.000	2.914	(1.039)	0.505	(0.206)	0.503	(0.220)	0.005	(0.197)	0.213	0.016	0.131
1999	9	9	1.000	2.923	(1.048)	0.524	(0.227)	0.576	(0.263)	−0.105	(0.150)	0.999	0.007	0.073
2001	13	11	0.846	3.233	(1.317)	0.541	(0.232)	0.523	(0.232)	0.033	(0.176)	0.926	−0.003	0.203
2003	8	8	1.000	3.079	(1.273)	0.522	(0.257)	0.489	(0.241)	0.069	(0.221)	0.733	0.000	0.237
2004	6	6	1.000	3.421	(1.222)	0.561	(0.241)	0.505	(0.213)	0.110	(0.178)	0.987	0.001	0.717
2006	7	6	0.833	2.786	(1.304)	0.497	(0.273)	0.508	(0.339)	−0.024	(0.276)	0.796	−0.017	0.022
2007	15	14	0.929	3.339	(1.257)	0.547	(0.224)	0.547	(0.206)	0.000	(0.171)	0.806	−0.002	0.099
2008	29	28	0.964	3.083	(1.196)	0.516	(0.236)	0.506	(0.229)	0.020	(0.096)	0.972	0.008	0.160
2009*a*	26	26	1.000	3.217	(1.068)	0.549	(0.192)	0.489	(0.180)	0.110	(0.122)	0.014	0.002	0.124
2009*b*	23	20	0.864	3.191	(1.239)	0.542	(0.212)	0.497	(0.183)	0.086	(0.144)	0.633	0.016	0.231
2011*a*	30	30	1.000	3.149	(1.073)	0.534	(0.203)	0.519	(0.207)	0.028	(0.164)	0.440	0.004	0.316
2011*b*	22	21	0.952	3.107	(0.923)	0.545	(0.189)	0.544	(0.225)	0.002	(0.226)	0.157	0.004	0.153
Overall	277	255	0.920	3.151	(1.072)	0.538	(0.204)	0.503	(0.187)	0.065	(0.073)	0.436	−0.037	0.231
Wild samples														
2008	69	63	0.912	3.300	(0.91)	0.575	(0.186)	0.558	(0.187)	0.030	(0.093)	0.554	−0.001	0.131
2009	60	60	1.000	3.273	(0.955)	0.558	(0.192)	0.552	(0.200)	0.012	(0.103)	0.324	−0.004	0.363
2011	44	42	0.953	3.399	(0.952)	0.580	(0.171)	0.555	(0.165)	0.044	(0.096)	0.074	−0.002	0.262
Overall	173	165	0.953	3.322	(0.932)	0.571	(0.182)	0.555	(0.179)	0.028	(0.061)	0.160	−0.003	0.131

P values for departure from equilibrium were corrected for multiple tests (*, *Q*value <0.01; **, *Q*value <0.001; ***, *Q*value <0.0001).
†Samples gathering individuals from different locations.

(Fig. S3, Supporting information; $P < 0.05$). This change through time in allelic frequencies was accompanied by an increase in genetic diversity through years (Fig. 5). This was particularly obvious for allelic richness, *A*r, but the same trend could also be observed for gene diversity, H_E. Within a few years, the cultivated population showed an increase in *A*r from 2.5 to 3, and from 0.44 to 0.53 for H_E. Interestingly, this evolution in genetic diversity ranged from the level observed for the fossil samples (at the lower bound in earlier cultivated samples) to level of the genetic diversity found within the wild population (upper bound reached since 2005). Moreover, examination of this temporal pattern revealed that the increase in genetic diversity was only evident after a time lag of four years – from 1994 to 1998 allelic richness, *A*r, was stable and gene diversity, H_E, displayed a slight decrease. Altogether, the pattern of variation in the population genetic indices provided several pieces of evidence that the cultivated population experienced a bottleneck followed by strong demographic expansion.

Discussion

While the rapid pace of pathogen evolution thwarts the development of sustainable crop protection strategies, it also provides opportunities to document evolutionary processes at work (McDonald 2010). At the same time, this accelerated evolution presents a challenge to the design of sampling schemes for studies of population

© 2016 John Wiley & Sons Ltd

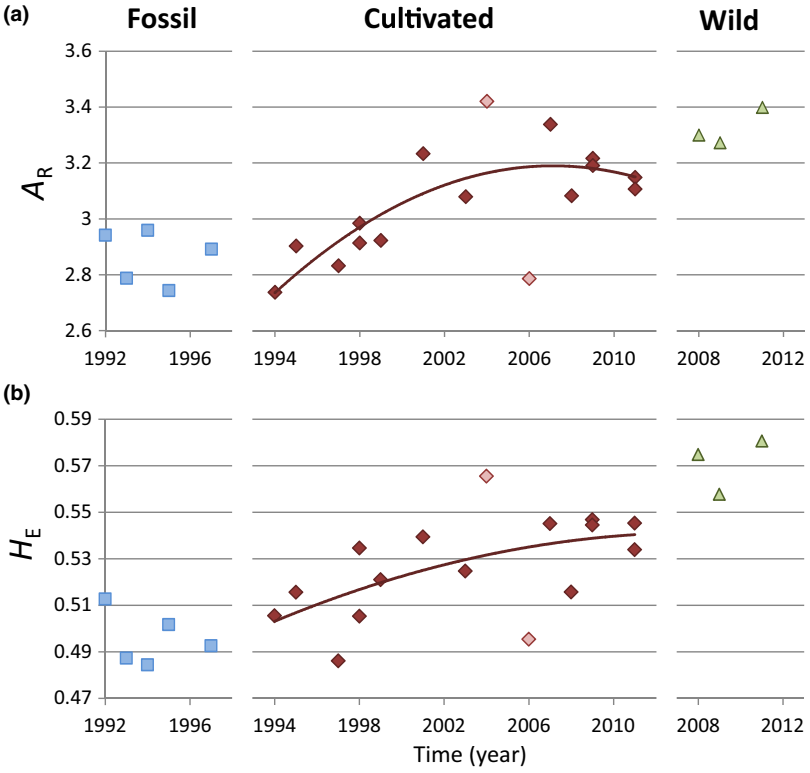

Fig. 5 Temporal evolution of neutral genetic diversity: (a) allelic richness (A_R); (b) gene diversity (H_E). Populations are sorted according to the three genetic groups identified by TESS analysis: the fossil, cultivated and wild populations, respectively, in blue, red and green. The two samples with the smallest sample size (cultivated population) are figured by faded diamond dots. [Colour figure can be viewed at wileyonlinelibrary.com]

genetic structure. In our study, the initial population that predominated before the R7 resistance breakdown would have remained unnoticed (as in Xhaard *et al.* 2011) without temporal sampling. Previous evolutionary studies have highlighted the added value of temporal analysis of phenotypic variation to decipher host–parasite co-evolution (Decaestecker *et al.* 2007; Gaba & Ebert 2009) and the dynamics of adaptation (Blanquart & Gandon 2013). Our population genetic analysis further exemplifies how temporal sampling can provide much more detailed insights into the demographic history of pathogen populations. Here, using both temporal records of virulence profiles and temporal population genetic data, our analyses revealed that (i) R7 resistance breakdown resulted in the emergence of a unique and homogeneous genetic group, the cultivated population, which predominated in northern France for about 20 years, (ii) selection for Vir7 individuals brought with it multiple other virulence types via hitchhiking, resulting in an overall increase in the population-wide number of virulence types and (iii) – above all – the drastic demographic expansion of the cultivated population leads to the extinction of the fossil population which predominated at the same place before R7 resistance breakdown. Our temporal analysis thus provides direct evidence that antagonistic co-evolution can lead to population extinction, hence providing definite support for the escalation hypothesis causing Red Queen dynamics.

Evidence for population replacement following an arms race scenario

The main finding of this study was the discovery of a fossil genetic group. Nearly all early samples collected in northern France clustered in a distinct ancestral population, which vanished after the R7 resistance breakdown. No individual was assigned to this population after 1998. Conversely, contemporaneous sampling indicated a homogeneous repartition of the cultivated population in all the cultivated poplar areas (Xhaard *et al.* 2011). Moreover, despite a comprehensive sampling of more than 1000 individuals collected in 2009 from 23 locations in France – analysed with the same set of microsatellite markers – Xhaard *et al.* (2011) did not find any trace of this fossil population. Lineages from this population may have persisted elsewhere in Europe, but in France, this population fully disappeared from contemporary samples.

The disappearance of the fossil population coincided with the collapse of Avr7 individuals in Nancy as this location was invaded by Vir7 individuals (hence the cultivated population). R7 resistance breakdown has led to major changes in the initial polymorphism both at neutral genetic markers (population replacement leading to the predominance of the cultivated population) and at virulence profiles (near fixation of Vir7 and hitchhiking of most other virulence types). Determining

© 2016 John Wiley & Sons Ltd

the conditions that lead to stable or transient polymorphism in gene-for-gene interactions (trench warfare vs. arms race models, respectively) has been the goal of a comprehensive body of theoretical literature (reviewed in Brown & Tellier 2011). Many factors can promote stable polymorphism, provided that they cause negative direct frequency-dependent selection (ndFDS) on either host or parasite populations. Host perenniality is one of these factors (Tellier & Brown 2009) because (i) it buffers the oscillation of resistance alleles thus retaining the 'memory' of past selective events and (ii) complex epidemiological dynamics are generated whereby host and parasite population sizes may vary drastically over time as a consequence and determinant of allele frequency changes (the so-called epidemiological feedback, Boots *et al.* 2014). These mechanisms stabilize allele frequencies around the equilibrium point. In the poplar rust system, hosts are perennials and thus expected to generate rather long-term polymorphism at the co-evolving loci. However, human management has created large genetically homogeneous host populations, and annual epidemics generate large allo-infections and rapid spread of disease within and between populations. These additional factors decrease ndFDS. They thwart perenniality in stabilizing the system and cause an arms race dynamic to occur, generating the conditions for population extinction. The population replacement in *M. larici-populina* illustrates our inability to eradicate pathogens via the simplistic control strategy of the sustained and massive deployment of a single resistance type. This strategy inevitably results in a strong selection pressure and destabilizes initial polymorphism in the pathogen population, even in a host–parasite couple that would otherwise be conducive for trench warfare stabilization of genetic polymorphism.

Admittedly, our observation of arms race escalation occurs in an anthropogenic environment which may not be typical of a natural co-evolution scenario (Van Valen 1973; Dawkins & Krebs 1979; Brockhurst *et al.* 2014). We think, nonetheless, that these results provided useful insights (i) to understand the consequences of human-mediated plant breeding on crop pathogen population dynamics, but also (ii) to inform our understanding of natural co-evolution in wild species with small population sizes. Co-evolutionary cycles do occur in agricultural systems, even if they are mediated by human decision. Numerous examples provide evidence that increasing the use of a resistance allele (i.e. frequency of resistance in a landscape) is followed by selection for virulence in the pathogen population, which in return decreases the usage of the resistance by breeders/farmers, and finally decreases the frequency of virulence in the pathogen population (McDonald 2010; Brown 2015). Our study provides a zoom into a small time window in which humans generated extremely strong selection by the wide deployment of the R7 allele in the poplar landscape, to such an extent that the arms race was out of human control. This evolutionary process is the same as expected *in natura* under the escalatory Red Queen scenario (Brockhurst *et al.* 2014). In addition, theoretical models show that the speed and amplitude of arms race dynamics depend not just on the co-evolutionary parameters of the interaction (especially the cost of the host of being infected) but also on the host and pathogen population mutation rates (Tellier *et al.* 2014). Very fast and complete fixation of resistance can occur in small host populations (<1000 diploid individuals), which in turn leads to the rapid fixation of virulence (Tellier *et al.* 2014), and to the pathogen population replacement, as proposed by Van Valen. Thus, even if an arms race scenario with very high-resistance allele frequency in the host population may not be typical of wild systems, especially for perennial hosts (Tellier & Brown 2009), these types of extreme dynamics with population replacement can occur in nature. Yet, they may be more difficult to highlight due to the lack of adequate temporal sampling of host and pathogen populations.

Origin of the cultivated population

Notably, our analysis pointed to a strict coincidence of the date of R7 resistance breakdown in 1994 and the date of the first detection of the cultivated population in France. In addition, all individuals sampled in 1994 on R7 cultivars – the first individuals bearing Vir7 – were convincingly assigned to the cultivated population. Moreover, those earliest samples in 1994 displayed narrow genotypic diversity and the same virulence profile (Pinon *et al.* 1998). We can thus confidently assess that the cultivated population was at the origin of R7 resistance breakdown. This population rapidly predominated in *M. larici-populina* samples, and – in accordance with our previous study (Xhaard *et al.* 2011) – formed the major contribution to contemporary samples of poplar rust. The continuity of assignments over 18 years denoted that the R7 resistance breakdown resulted from a single event of virulence emergence. However, the fact that we observed some diversity in genotypic and virulence profiles in the very first individuals bearing Vir7 suggests that the R7 resistance breakdown took place sometime before 1994 (Pinon & Frey 2005). Indeed, if samples had been collected the year of resistance breakdown, they would have consisted in the same clonal lineage, as they would have reproduced only asexually on poplars. Here, one or two annual events of sexual reproduction on larch are likely

© 2016 John Wiley & Sons Ltd

to have generated the level of genotypic diversity observed in the 1994 sampling.

Based on the examination of virulence profiles, we can further postulate that cultivated individuals likely originated from the fossil population, as they shared many virulence types (except virulence 7). Wild individuals, in contrast, display less complex virulence profiles. On top of that, the main virulence profile of the cultivated individuals (1-3-4-5-7) was already present within the fossil population (1-3-4-5) but was totally absent from the wild population. The inference that cultivated individuals originated from the fossil population is in accordance with our observation that both populations existed in sympatry at the time of R7 resistance breakdown. As the very first Vir7 isolates were detected in Belgium and nearby in northern France, resistance breakdown likely took place in this area (Pinon *et al.* 1998). However, as rust species are well known for their long-distance migration capacities (Brown & Hovmøller 2002; Barrès *et al.* 2008; Ali *et al.* 2014), we cannot exclude the possibility that virulent individuals migrated from a distinct source. Unfortunately, due to gene reshuffling during sexual reproduction, it is difficult to keep track of the fate of individual MLGs across time and space as is done for asexual species (Ali *et al.* 2014; Hovmøller *et al.* 2016).

Expansion and diversification of the cultivated population

The variation of population genetic indices along the temporal samples of the cultivated population provided further insights on the demographic changes accompanying its emergence and spread. In particular, we found that the 1994 sample displayed a reduced genetic diversity compared with later samples, as well as strong genetic disequilibria (significant deviations from Hardy–Weinberg proportions, expected heterozygosity and linkage across loci). Such hallmarks of a founder effect following resistance breakdown have previously been observed in several pathogen species. The best illustrated example concerns the apple scab fungus, *Venturia inaequalis* (Guérin & Le Cam 2004; Guérin *et al.* 2007; Gladieux *et al.* 2011). These authors reported a reduced genetic diversity (Guérin & Le Cam 2004) and strong genetic differentiation between individuals sampled on susceptible or resistant cultivars, even if collected in the same orchard (Leroy *et al.* 2013). Although this species reproduces sexually, the levels of genetic diversity and differentiation remained stable through years, with only few hybrids detected (Gladieux *et al.* 2011). This provided evidence for strong reproductive isolation between individuals evolving on either susceptible or resistant cultivars (Gladieux *et al.* 2011). Interestingly, in this example the native population persists, even co-existing in sympatry with the emerging population (Gladieux *et al.* 2011; Leroy *et al.* 2013), which was not the case in *M. larici-populina*.

In our study, the cultivated population quickly returned to equilibrium with no significant deviation as early as 1995. This fast disappearance of the bottleneck signal is likely due to the obligate annual sexual reproduction on larch. The fact that individuals disperse over long distances and mate at common places increases the reshuffling of alleles (Barrès *et al.* 2008; Gilabert *et al.* 2009). Other biological systems can retain the signatures of demographic events for longer periods, such as by germ banking via seed or insect dormancy, which keeps the signatures of ancient population decline for a much longer time (Živković & Tellier 2012). The obligate sexual reproduction and host alternation in *M. larici-populina* maximizes the effect of recombination and thus rapidly erases any trace of changes in population size. This does not mean, however, that asexual reproduction had no role in the establishment and evolutionary success of the cultivated population. The alternation in sexual and asexual reproduction accelerates the pace of adaptation (McDonald & Linde 2002), with – on the one hand – sexual reproduction that generates diversity (the fuel for adaptive evolution) and – on the other hand – asexual multiplication that increases the strength of selection through the amplification of the evolutionary success of the fittest genotype(s). In our analysis, we indeed found some repeated genotypes in the earliest sample of the cultivated population despite our limited sample size, indicating that *M. larici-populina* benefited from asexual reproduction at least for the establishment of the first Vir7 individuals.

The temporal analysis showed a sustained increase in genetic diversity of the cultivated population as it spread through time. The genetic diversity of the cultivated population started from the level observed in the fossil samples and climbed to reach the higher level observed for wild samples. Conversely, Gladieux *et al.* (2011) found no significant increase in allelic richness across years in samples of the apple scab pathogen *V. inaequalis*. Our observation of a temporal increase in genetic diversity also contrasts with pattern observed for host tracking pathogens, which often display a reduction in diversity as they spread away from the centre of domestication of the host plant (Gladieux *et al.* 2008; Bahri *et al.* 2009b; Ali *et al.* 2014; Saleh *et al.* 2014), and as is commonly found in phylogeographic studies of range expansion (Petit *et al.* 1997; Excoffier *et al.* 2009). These discrepancies may arise because of a difference in geneflow regimes between endemic and virulent/spreading populations. The populations of *V. inaequalis* have been shown to be reproductively

© 2016 John Wiley & Sons Ltd

isolated (Gladieux *et al.* 2011) and theoretical models of range expansion often assume that invading species have their own ecological niche where they can reproduce (Excoffier *et al.* 2009). In our system, the host-alternating life cycle of *M. larici-populina* increases the probability of gene mixing between cultivated individuals and other genetic groups (wild and fossil populations). Irrespective of their population of origin, all individuals attended the mating rendezvous on larch. As a result, pronounced gene mixing leads to genetic homogenization towards the most predominant population (*i.e.* the cultivated individuals, which can multiply on all hosts including the predominantly planted R7 cultivars), and to increased genetic diversity as the cultivated population spread throughout France and mixed, first with the fossil individuals, then with the wild individuals.

Concluding remarks: How did the Red Queen kill the blue King?

The coexistence (even ephemeral) of pure cultivated and fossil genotypes observed between 1994 and 1998 is puzzling. How did genetic differentiation arise between sympatric fossil and cultivated genotypes? And how could the predominant fossil population have been driven to extinction so quickly, without leaving much genetic background in the cultivated population? If a single (dominant) allele was selected for, we would have observed a selective sweep within the fossil population, not the emergence of the incipient cultivated population.

We posit that the differentiation could have arisen from the peculiarities of the gene-for-gene system and a cost of virulence of the *vir7* allele. *Melampsora larici-populina* is dikaryotic (i.e. diploid) and following the gene-for-gene model (Flor 1971; Brown & Tellier 2011), the virulence allele should be recessive. Thus, the individuals which caused R7 resistance breakdown were homozygous *vir7*/*vir7*. They could have mated with Avr7 individuals on larch, but their progeny would then be heterozygous *vir7*/*Avr7*, and avirulent on R7 cultivars. Hence, the incipient cultivated population – that was strongly selected for by the wide planting of R7 poplars – mainly resulted from mating among a given class of individuals on larch (only the homozygotes *vir7*/*vir7*). Indeed, mating predominantly among incipient cultivated genotypes is in accordance with the elevated level of F_{IS} found in the first two cultivated samples. The differentiation was thus not caused by direct assortative mating (as may be the case for *V. inaequalis*, Gladieux *et al.* 2011), but would rather have resulted from postzygotic differential success. Heterozygous individuals may have also existed, but they would have suffered from a twofold fitness penalty compared with the homozygous individuals: (i) unlike *vir7*/*vir7* individuals, heterozygotes could not invade R7 cultivars, and had thus no selective advantage; and (ii) assuming that bearing the vir7 allele was costly, heterozygotes would have had a reduced performance on susceptible hosts compared with *Avr7*/*Avr7* homozygous individuals. According to this scenario, the incipient cultivated population might have been founded and remained differentiated despite there being no biological barrier to mating between the two populations. These two populations lived in direct interaction and it was indeed selection exerted by the host population which drove the fossil population to extinction and to its replacement by the cultivated individuals, in accordance with Van Valen's evolutionary law (Van Valen 1973). In the near future, we will pursue our investigation on the population replacement in *M. larici-populina* using population genomics approaches and evolutionary quantitative genetics to decipher the tempo of adaptation and the genomic signature following the extreme selective event of a parasite running with the Red Queen.

Acknowledgements

The authors are grateful to Jean Pinon who initiated poplar rust population sampling and virulence typing at INRA Nancy in the 1980s. Without his pioneer work, this study would not have been possible. Axelle Andrieux is acknowledged for her excellent technical help in genotyping. We thank Sébastien Duplessis, Pierre Gladieux, Martin Lascoux and Christophe Lemaire for valuable comments on an earlier draft of this manuscript. This manuscript also benefited from constructive comments by the subject editor, Tatiana Giraud, and three anonymous reviewers. This work was supported by grants from the French National Research Agency (ANR-13-BSV7-0011, FunFit project; ANR-12-ADAP-0009, GANDALF project, ANR-11-BSV7-0007, Clonix project). The IAM Laboratory forms part of Cluster of Excellence ARBRE (ANR-11-LABX-0002-01). A. Persoons was supported by a PhD fellowship from the Région Lorraine and INRA. K.J. Hayden was supported by a postdoctoral fellowship from the INRA MetaProgramme SMaCH and the AgreenSkills Mobility Program (Grant Agreement PCOFUND-GA-2010-267196).

References

Agapow P-M, Burt A (2001) Indices of multilocus linkage disequilibrium. *Molecular Ecology Notes*, **1**, 101–102.

Ali S, Gladieux P, Leconte M *et al.* (2014) Origin, migration routes and worldwide population genetic structure of the wheat yellow rust pathogen *Puccinia striiformis* f.sp. *tritici*. *PLoS Pathogens*, **10**, e1003903.

Andrivon D, De Vallavieille-Pope C (1995) Race diversity and complexity in selected populations of fungal biotrophic pathogens of cereals. *Phytopathology*, **85**, 897.

© 2016 John Wiley & Sons Ltd

Bahri B, Kaltz O, Leconte M, de Vallavieille-Pope C, Enjalbert J (2009a) Tracking costs of virulence in natural populations of the wheat pathogen, *Puccinia striiformis* f.sp. *tritici*. *BMC Evolutionary Biology*, **9**, 26.

Bahri B, Leconte M, Ouffroukh A, De Vallavieille-Pope C, Enjalbert J (2009b) Geographic limits of a clonal population of wheat yellow rust in the Mediterranean region. *Molecular Ecology*, **18**, 4165–4179.

Barrès B, Halkett F, Dutech C *et al.* (2008) Genetic structure of the poplar rust fungus *Melampsora larici-populina*: evidence for isolation by distance in Europe and recent founder effects overseas. *Infection, Genetics and Evolution*, **8**, 577–587.

Barrès B, Dutech C, Andrieux A, Halkett F, Frey P (2012) Exploring the role of asexual multiplication in poplar rust epidemics: impact on diversity and genetic structure. *Molecular Ecology*, **21**, 4996–5008.

Belkhir K, Borsa P, Chikhi L, Raufaste N, Bonhomme F (1996-2004) *GENETIX 4.05, Logiciel Sous Windows TM Pour La Génétique Des Populations*. Laboratoire Génome, Populations, Interactions, CNRS UMR 5171, Université de Montpellier II, Montpellier (France).

Benjamini Y, Yekutieli D (2001) The control of the false discovery rate in multiple testing under dependency. *The Annals of Statistics*, **29**, 1165–1188.

Betts A, Kaltz O, Hochberg ME (2014) Contrasted coevolutionary dynamics between a bacterial pathogen and its bacteriophages. *Proceedings of the National Academy of Sciences of the United States of America*, **111**, 11109–11114.

Blanquart F, Gandon S (2013) Time-shift experiments and patterns of adaptation across time and space. *Ecology Letters*, **16**, 31–38.

Boots M, White A, Best A, Bowers R (2014) How specificity and epidemiology drive the coevolution of static trait diversity in hosts and parasites. *Evolution*, **68**, 1594–1606.

Brockhurst MA, Chapman T, King KC *et al.* (2014) Running with the Red Queen: the role of biotic conflicts in evolution. *Proceedings of the Royal Society B: Biological Sciences*, **281**, 20141382.

Brown JKM (2015) Durable resistance of crops to disease: a Darwinian perspective. *Annual Review of Phytopathology*, **53**, 513–539.

Brown JKM, Hovmøller MS (2002) Aerial dispersal of pathogens on the global and continental scales and its impact on plant disease. *Science*, **297**, 537–541.

Brown JKM, Tellier A (2011) Plant-parasite coevolution: bridging the gap between genetics and ecology. *Annual Review of Phytopathology*, **49**, 345–367.

Busch JW, Neiman M, Koslow JM (2004) Evidence for maintenance of sex by pathogens in plants. *Evolution*, **58**, 2584–2590.

Chen C, Durand E, Forbes F, François O (2007) Bayesian clustering algorithms ascertaining spatial population structure: a new computer program and a comparison study. *Molecular Ecology Notes*, **7**, 747–756.

Cornuet JM, Luikart G (1996) Description and power analysis of two tests for detecting recent population bottlenecks from allele frequency data. *Genetics*, **144**, 2001–2014.

Dawkins R, Krebs JR (1979) Arms races between and within species. *Proceedings of the Royal Society of London B: Biological Sciences*, **205**, 489–511.

Decaestecker E, Gaba S, Raeymaekers JAM *et al.* (2007) Host–parasite "Red Queen" dynamics archived in pond sediment. *Nature*, **450**, 870–873.

Durand E, Jay F, Gaggiotti OE, Francois O (2009) Spatial inference of admixture proportions and secondary contact zones. *Molecular Biology and Evolution*, **26**, 1963–1973.

Dybdahl MF, Lively CM (1998) Host-parasite coevolution: evidence for rare advantage and time-lagged selection in a natural population. *Evolution*, **52**, 1057.

Evanno G, Regnaut S, Goudet J (2005) Detecting the number of clusters of individuals using the software STRUCTURE: a simulation study. *Molecular Ecology*, **14**, 2611–2620.

Excoffier L, Foll M, Petit RJ (2009) Genetic consequences of range expansions. *Annual Review of Ecology, Evolution, and Systematics*, **40**, 481–501.

Fager EW (1972) Diversity: a sampling study. *The American Naturalist*, **106**, 293–310.

Flor HH (1971) Current status of the gene-for-gene concept. *Annual Review of Phytopathology*, **9**, 275–296.

Frey P, Gérard PR, Feau N, Husson C, Pinon J (2005) Variability and population biology of *Melampsora* rusts on poplars. In: *Rust Diseases of Willow and Poplar* (eds Pei MH, McCraken AR), pp. 63–72. CAB International, Wallingford, UK.

Gaba S, Ebert D (2009) Time-shift experiments as a tool to study antagonistic coevolution. *Trends in Ecology & Evolution*, **24**, 226–232.

Gérard PR, Husson C, Pinon J, Frey P (2006) Comparison of genetic and virulence diversity of *Melampsora larici-populina* populations on wild and cultivated poplar and influence of the alternate host. *Phytopathology*, **96**, 1027–1036.

Gilabert A, Simon J-C, Mieuzet L *et al.* (2009) Climate and agricultural context shape reproductive mode variation in an aphid crop pest. *Molecular Ecology*, **18**, 3050–3061.

Gladieux P, Zhang X-G, Afoufa-Bastien D *et al.* (2008) On the origin and spread of the scab disease of apple: out of Central Asia. *PLoS ONE*, **3**, e1455.

Gladieux P, Guérin F, Giraud T *et al.* (2011) Emergence of novel fungal pathogens by ecological speciation: importance of the reduced viability of immigrants. *Molecular Ecology*, **20**, 4521–4532.

Goudet J (1995) FSTAT (Version 1.2): a computer program to calculate *F*-statistics. *Journal of Heredity*, **86**, 485–486.

Guérin F, Le Cam B (2004) Breakdown of the scab resistance gene Vf in apple leads to a founder effect in populations of the fungal pathogen *Venturia inaequalis*. *Phytopathology*, **94**, 364–369.

Guérin F, Gladieux P, Le Cam B (2007) Origin and colonization history of newly virulent strains of the phytopathogenic fungus *Venturia inaequalis*. *Fungal Genetics and Biology*, **44**, 284–292.

Halkett F, Simon J, Balloux F (2005) Tackling the population genetics of clonal and partially clonal organisms. *Trends in Ecology & Evolution*, **20**, 194–201.

Hendry AP, Day T (2005) Population structure attributable to reproductive time: isolation by time and adaptation by time. *Molecular Ecology*, **14**, 901–916.

Hovmøller MS, Walter S, Bayles RA *et al.* (2016) Replacement of the European wheat yellow rust population by new races from the centre of diversity in the near-Himalayan region. *Plant Pathology*, **65**, 402–411.

Huang Y-J, Li Z-Q, Evans N *et al.* (2006) Fitness cost associated with loss of the AvrLm4 avirulence function in *Leptosphaeria maculans* (Phoma Stem Canker of Oilseed Rape). *European Journal of Plant Pathology*, **114**, 77–89.

© 2016 John Wiley & Sons Ltd

Jombart T, Collins C (2015) *A tutorial for discriminant analysis of principal components (DAPC) using adegenet 2.0*. MRC Centre for Outbreak Analysis and Modelling, Imperial College London, London.

Jombart T, Devillard S, Balloux F (2010) Discriminant analysis of principal components: a new method for the analysis of genetically structured populations. *BMC Genetics*, **11**, 1.

Jones JDG, Dangl JL (2006) The plant immune system. *Nature*, **444**, 323–329.

Leroy T, Lemaire C, Dunemann F, Le Cam B (2013) The genetic structure of a *Venturia inaequalis* population in a heterogeneous host population composed of different *Malus* species. *BMC Evolutionary Biology*, **13**, 1.

Lively CM (2010) A review of Red Queen models for the persistence of obligate sexual reproduction. *Journal of Heredity*, **101**, S13–S20.

Lively CM, Craddock C, Vrijenhoek RC (1990) Red Queen hypothesis supported by parasitism in sexual and clonal fish. *Nature*, **344**, 864–866.

Luikart G, Cornuet J-M (1998) Empirical evaluation of a test for identifying recently bottlenecked populations from allele frequency data. *Conservation Biology*, **12**, 228–237.

McDonald BA (2010) How can we achieve durable disease resistance in agricultural ecosystems? *New Phytologist*, **185**, 3–5.

McDonald BA, Linde C (2002) Pathogen population genetics, evolutionary potential, and durable resistance. *Annual Review of Phytopathology*, **40**, 349–379.

Montarry J, Hamelin FM, Glais I, Corbière R, Andrivon D (2010) Fitness costs associated with unnecessary virulence factors and life history traits: evolutionary insights from the potato late blight pathogen *Phytophthora infestans*. *BMC Evolutionary Biology*, **10**, 1.

Nei M (1978) Estimation of average heterozygosity and genetic distance from a small number of individuals. *Genetics*, **89**, 583–590.

Petit RJ, Pineau E, Demesure B *et al*. (1997) Chloroplast DNA footprints of postglacial recolonization by oaks. *Proceedings of the National Academy of Sciences of the United States of America*, **94**, 9996–10001.

Pinon J, Frey P (2005) Interactions between poplar clones and *Melampsora* populations and their implications for breeding for durable resistance. In: *Rust diseases of willow and poplar* (eds Pei MH, McCraken AR), pp. 139–154. CAB International, Wallingford, UK.

Pinon J, Frey P, Husson C, Schipfer A (1998) Poplar rust (*Melampsora larici-populina*): the development of E4 pathotypes in France since 1994. In: *Proceedings of the First IUFRO Rusts of Forest Trees Conference, Saariselkä, Finland* (eds Jalkanen R, Crane PE, Walla JA, Aalto T), pp. 57–64. Finnish Forest Research Institute, Research Paper 712, Saarijärvi.

Piry S, Luikart G, Cornuet JM (1999) Computer note. BOTTLENECK: a computer program for detecting recent reductions in the effective size using allele frequency data. *Journal of Heredity*, **90**, 502–503.

Poppe S, Dorsheimer L, Happel P, Stukenbrock EH (2015) Rapidly evolving genes are key players in host specialization and virulence of the fungal wheat pathogen *Zymoseptoria tritici* (*Mycosphaerella graminicola*). *PLOS Pathogens*, **11**, e1005055.

R Core Team (2014) *R: A Language and Environment for Statistical Computing*. R Foundation for Statistical Computing, Vienna, Austria.

Rouger R, Reichel K, Malrieu F, Masson JP, Stoeckel S (2016) Effects of complex life cycles on genetic diversity: cyclical parthenogenesis. *Heredity*, **117**, 336–347.

Rousset F (1997) Genetic differentiation and estimation of gene flow from *F*-statistics under isolation by distance. *Genetics*, **145**, 1219–1228.

Rousset F (2008) GENEPOP'007: a complete re-implementation of the GENEPOP software for Windows and Linux. *Molecular Ecology Resources*, **8**, 103–106.

Saleh D, Milazzo J, Adreit H, Fournier E, Tharreau D (2014) South-East Asia is the center of origin, diversity and dispersion of the rice blast fungus, *Magnaporthe oryzae*. *New Phytologist*, **201**, 1440–1456.

Schulze-Lefert P, Peterhaensel C, Freialdenhoven A (1997) Mutation analysis for the dissection of resistance. In: *The Gene-for-Gene Relationship in Plant-Parasite Interactions* (eds Crute IR, Holub EB, Burdon JJ), pp. 45–63. CAB International, New York.

Spiegelhalter DJ, Best NG, Carlin BP, van der Linde A (2002) Bayesian measures of model complexity and fit. *Journal of the Royal Statistical Society Series B (Statistical Methodology)*, **64**, 583–639.

Storey JD, Tibshirani R (2003) Statistical significance for genomewide studies. *Proceedings of the National Academy of Sciences of the United States of America*, **100**, 9440–9445.

Tellier A, Brown JK (2007) Stability of genetic polymorphism in host-parasite interactions. *Proceedings of the Royal Society B: Biological Sciences*, **274**, 809–817.

Tellier A, Brown JKM (2009) The influence of perenniality and seed banks on polymorphism in plant-parasite interactions. *The American Naturalist*, **174**, 769–779.

Tellier A, Moreno-Gámez S, Stephan W (2014) Speed of adaptation and genomic footprints of host-parasite coevolution under arms race and trench warfare dynamics. *Evolution*, **68**, 2211–2224.

Thrall PH, Burdon JJ, Young A (2001) Variation in resistance and virulence among demes of a plant host–pathogen metapopulation. *Journal of Ecology*, **89**, 736–748.

Thrall PH, Laine A-L, Ravensdale M *et al*. (2012) Rapid genetic change underpins antagonistic coevolution in a natural host-pathogen metapopulation: coevolution in a wild host-pathogen system. *Ecology Letters*, **15**, 425–435.

Van Valen L (1973) A new evolutionary law. *Evolutionary Theory*, **1**, 1–30.

Vialle A, Frey P, Hambleton S, Bernier L, Hamelin RC (2011) Poplar rust systematics and refinement of *Melampsora* species delineation. *Fungal Diversity*, **50**, 227–248.

Weir BS, Cockerham CC (1984) Estimating *F*-statistics for the analysis of population structure. *Evolution*, **38**, 1358–1370.

Xhaard C, Andrieux A, Halkett F, Frey P (2009) Characterization of 41 microsatellite loci developed from the genome sequence of the poplar rust fungus, *Melampsora larici-populina*. *Conservation Genetics Resources*, **1**, 21–25.

Xhaard C, Fabre B, Andrieux A *et al*. (2011) The genetic structure of the plant pathogenic fungus *Melampsora larici-populina* on its wild host is extensively impacted by host domestication. *Molecular Ecology*, **20**, 2739–2755.

Xhaard C, Barrès B, Andrieux A *et al*. (2012) Disentangling the genetic origins of a plant pathogen during disease spread using an original molecular epidemiology approach. *Molecular Ecology*, **21**, 2383–2398.

© 2016 John Wiley & Sons Ltd

Živković D, Tellier A (2012) Germ banks affect the inference of past demographic events. *Molecular Ecology*, **21**, 5434–5446.

A.P., P.F. and F.H. conceived and designed the study. A.P. purified the isolates when necessary and carried out the molecular genotyping and population genetic analyses. F.H. supervised the molecular genotyping. F.H. and S.D.M. supervised population genetic analyses. B.F. built the virulence type database. K.H. and F.H. performed the virulence type analyses. A.P., K.H. and F.H. prepared the manuscript. A.T. provided expertise on theoretical gene-for-gene evolution. All authors revised and approved the manuscript.

Data accessibility

Microsatellite data (594 individuals typed with 25 markers) and virulence profile data (6494 individuals phenotyped on a differential set of eight resistant poplars) are publicly available from Dryad repository: https://doi.org/10.5061/dryad.r6d8h.

Supporting information

Additional supporting information may be found in the online version of this article.

Data S1 Supplementary Information.

© 2016 John Wiley & Sons Ltd